The 11th Canadian Conference on Earthquake Engineering
Canadian Association for Earthquake Engineering

SEISMIC RESPONSE MODIFICATION FACTORS FOR GFRP-REINFORCED CONCRETE SHEAR WALLS

Nayera MOHAMED
Postdoctoral fellow, Department of Civil Engineering, University of Sherbrooke, Canada
Nayera.Mohamed@usherbrooke.ca

Ahmed Sabry FARGHALY
Postdoctoral fellow, Department of Civil Engineering, University of Sherbrooke, Canada
Ahmed.Farghaly@usherbrooke.ca

Brahim BENMOKRANE
Professor of Civil Engineering, and NSERC Research Chair in Innovative FRP Composite Reinforcements for Concrete Infrastructure and Tier-1 Canada Research Chair in Advanced Composite Materials for Civil Structures, Department of Civil Engineering, University of Sherbrooke, Canada
Brahim.Benmokrane@usherbrooke.ca

ABSTRACT: Experimental analysis of reinforced shear-wall with glass-fiber-reinforced polymer (GFRP) showed its applicability in resisting lateral loads with no strength degradation, while evidencing acceptable deformation capacity and energy dissipation, as illustrated in an earlier article by the authors. The observed performance of GFRP-reinforced shear walls strongly suggested the necessity of proposing a design procedure for such lateral-resisting members. Proposing design guidelines, however, require the determination elastic and inelastic deformation as well as an assessment of the force modification factor for GFRP-reinforced shear walls. Accordingly, methods for estimating the virtual yield for GFRP-reinforced shear walls and maximum allowable displacement were proposed with suggestions of appropriate definitions. The force modification factor was estimated based on the idealized curve of the tested GFRP-reinforced shear walls.

1. Introduction

The use of fiber-reinforced-polymer (FRP) bars has been growing to overcome deterioration owing to corrosion of steel reinforcement. Previous studies (Cardenas et al. 1973, Fintel 1995) indicated that well-designed shear walls have proven to provide excellent cost-effective lateral resistance in comparison to other lateral-resisting systems. An earlier experimental study by the authors (Mohamed et al. 2014) tested large-scale GFRP-reinforced shear walls, which evidenced acceptable performance in resisting lateral loads associated with adequate deformation capacity. The test results indicated that GFRP-reinforced shear walls can resist lateral loads in regions with low to moderate risk of earthquakes.

Accordingly, the primary guidelines for the seismic design of GFRP-reinforced shear walls need to be investigated. Assessing the design procedure, however, requires the generation of idealized curves and the determination of a value for the force reduction factor (Adebar et al. 2005). To account for deformability and energy-dissipation effect, most seismic design codes allow for a reduction in seismic forces calculated from elastic behavior. The *National Building Code of Canada* (NBCC 2010) derives the force modification factor from the ductility-related force modification factor (R_d) and the overstrength-related force modification factor (R_o). CSA S806 (2012) assumes a value of unity for both ductility- and overstrength-related force modification factors (R_d and R_o, respectively) for designing members reinforced with FRP bars. The suggested value (unity) is extremely conservative and was chosen due to lack of data for lateral-resisting systems reinforced with FRP bars. The authors, based on their recent experimental

results (Mohamed et al. 2014), suggest herein appropriate values for the seismic-response modification factors for GFRP-reinforced shear walls, while adopting the force-based seismic-design philosophies of NBCC (2010).

2. Summary of Experimental Program and Results

2.1. General

The experimental program comprised the testing to failure of four reinforced-concrete shear walls, including one reference steel-reinforced specimen (ST15) and three GFRP-reinforced specimens (G15, G12, and G10) under quasi-static loading. The specimens represent a model of a single medium-rise shear wall. The minimum thickness and reinforcement details for the steel-reinforced wall were designed according to CSA A23.3 (2004) and ACI 318 (2008), whereas CSA S806 (2012) and ACI 440.1R (2006) were used for the GFRP-reinforced walls, where applicable. Wall specimens were designed with an adequate amount of distributed and concentrated reinforcement to ensure flexural domination and to prevent shear, sliding shear, and anchorage failures. The wall specimens were all 3500 mm high (h_w) and 200 mm thick (b_w). ST15 and G15 were 1500 mm long (l_w). ST15 served as a reference for G15, since it had the same concrete dimensions and similar reinforcement axial stiffness. The lengths of G12 and G10 were 1200 mm and 1000 mm, respectively. Figure 1-a shows the concrete dimensions and reinforcement details of the GFRP-reinforced shear-walls, respectively. Figure 1-b provides the test setup. More details about shear-wall specimens can be found in Mohamed et al. (2014).

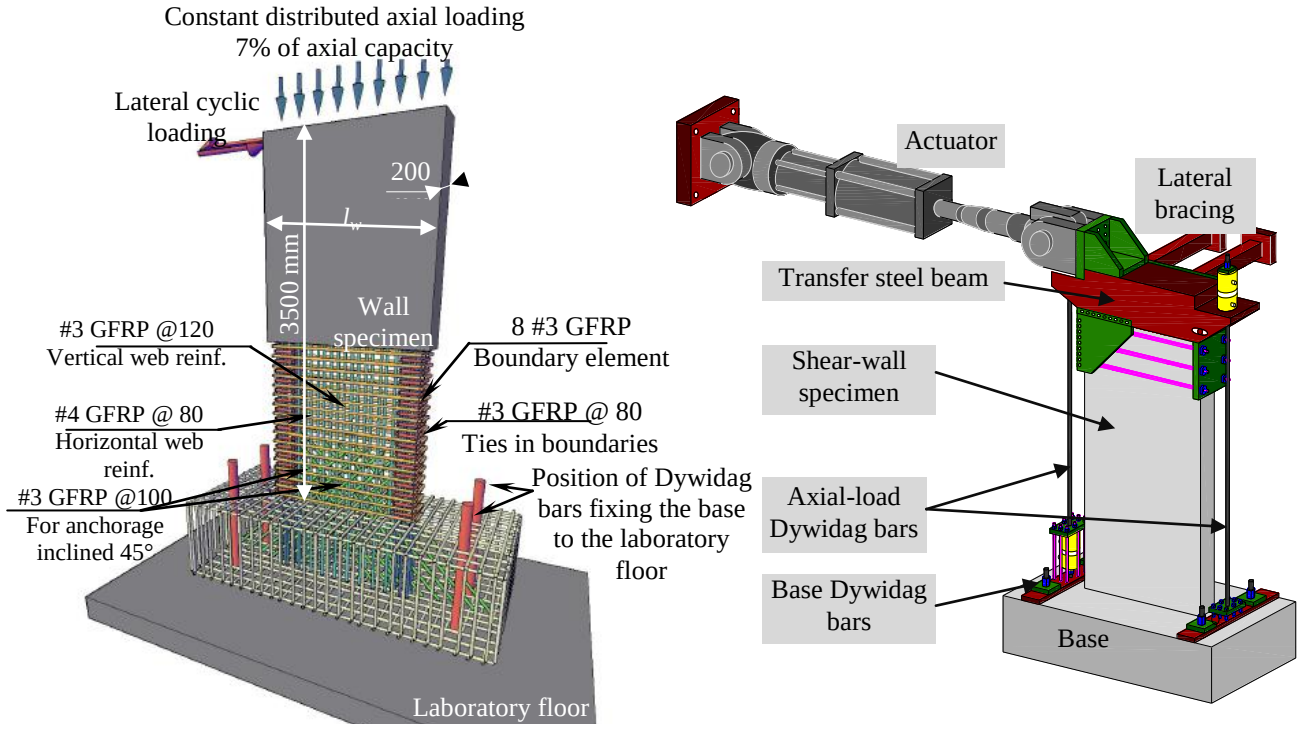

(a) Concrete dimensions and reinforcement details

(b) Test setup

Fig. 1 – Concrete Dimension, Reinforcement Details, and Test Setup

2.2. Hysteretic Response

Figure 2 gives the hysteretic curves for the tested walls. In the early stages, ST15 achieved a higher load than G15, due to the softened response of G15 up to a lateral drift of 2.1%, corresponding to 99% and 80% of ultimate load for ST15 and G15, respectively. After that point, G15 kept increasing almost linearly to failure. Failure was due to concrete crushing following buckling of the longitudinal steel bars in ST15 and was associated with longitudinal and transverse rupture of the GFRP bars in G15, G12, and G10.

The concrete cover of ST15 and G15 split—considered moderate damage—at similar loads but at different drift levels (464 kN and 456 kN) at lateral drifts of 1.43 % and 2% for ST15 and G15, respectively (Mohamed et al. 2014). The drift values attained with moderate damage to both walls fall within the range of 1.5% to 2.5%, which is the recommended design range for drift in many codes (Duffey et al. 1994).

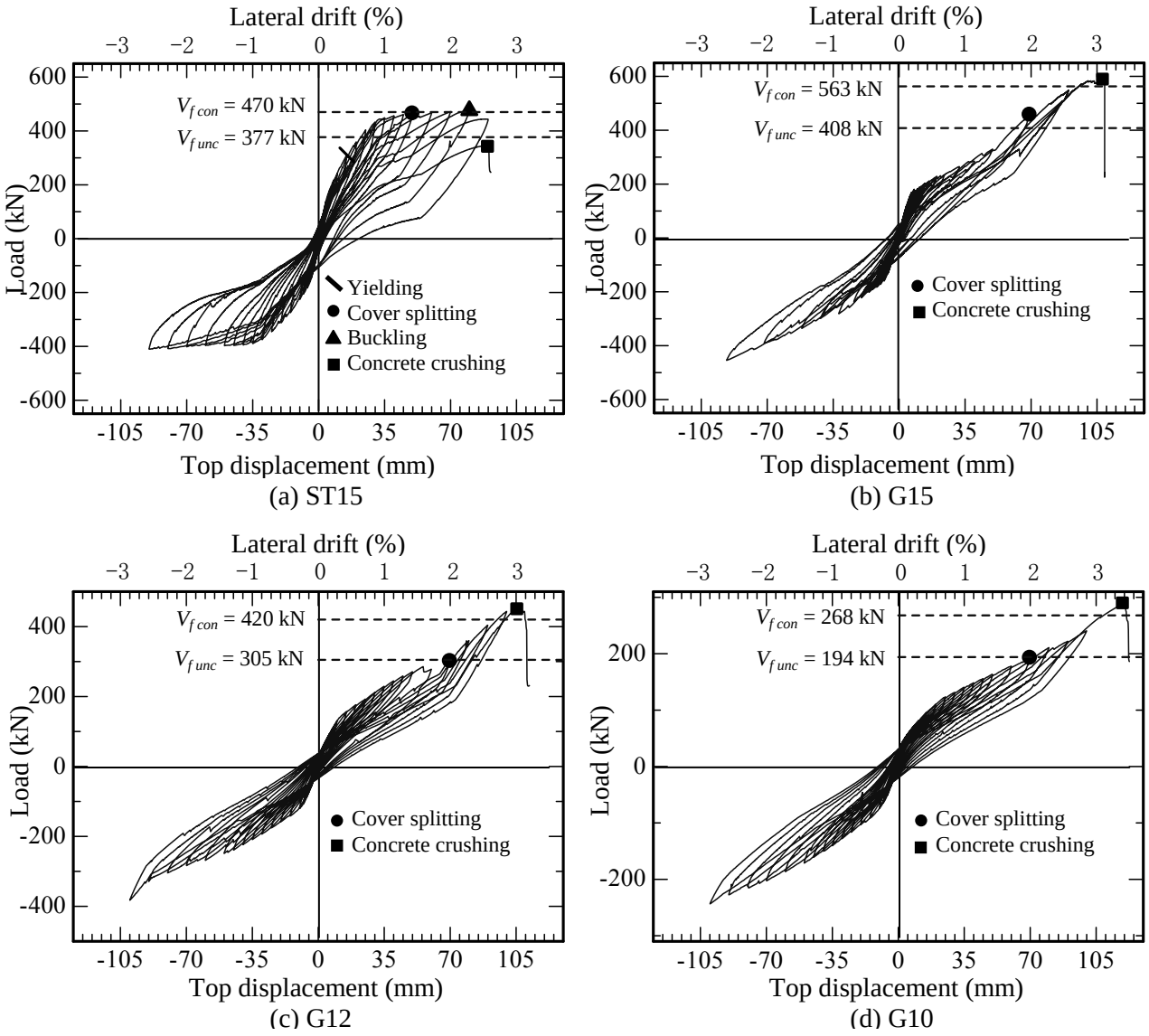

Fig. 2 – Lateral Load versus Top-Displacement Relationship (Mohamed et al. 2014)

2.3. Energy Dissipation

In addition to adequate drift level, energy-dissipation capacity is a desirable characteristic in shear-wall behavior. The energy-dissipation capacity of a member can be evaluated in various ways. Moreover, this capacity is recognized as an important parameter with respect to a structure's seismic performance. Although the accumulative dissipated energy when the structure fails is an important parameter, it does not clearly indicate the level of deformation at which this energy is dissipated. Furthermore, it is also subject to uncertainties in defining failure. On the other hand, the amount of energy dissipated at a given drift level allows for more meaningful comparisons between different structures. Nevertheless, it has to be supplemented by an indicator of the structure's residual force; otherwise, the picture is rather incomplete (Salonikios et al. 2000).

Figure 3-a shows the calculated dissipated energy at each cycle for the tested walls. For drifts less than 1%, the dissipated energy was quite small. For larger drifts, however, a nearly linear increase of the dissipated energy with respect to an increase in drift level can be observed. The steel-reinforced wall (ST15) had higher dissipated energy than the GFRP-reinforced walls. It is interesting to note that walls ST15 and G15 experienced similar energy dissipation (13 and 11 kN.m, respectively) at lateral drifts of 1.43% and 2%, respectively, corresponding to cover splitting, which is considered moderate damage. As the lateral load increased, ST15 experienced higher inelastic deformation than G15, yielding to higher dissipated energy in comparison to G15. Despite G15's pinched behavior, G15's greater strength in comparison to ST15 significantly contributed to its increased energy-dissipation capacity. The effect of aspect ratio was clear, since the walls with lower aspect ratios yielded higher dissipated energy, this due to their exhibiting higher ultimate capacity and relatively higher inelastic deformation (11, 7, and 5 kN.m for G15, G12, and G10, respectively).

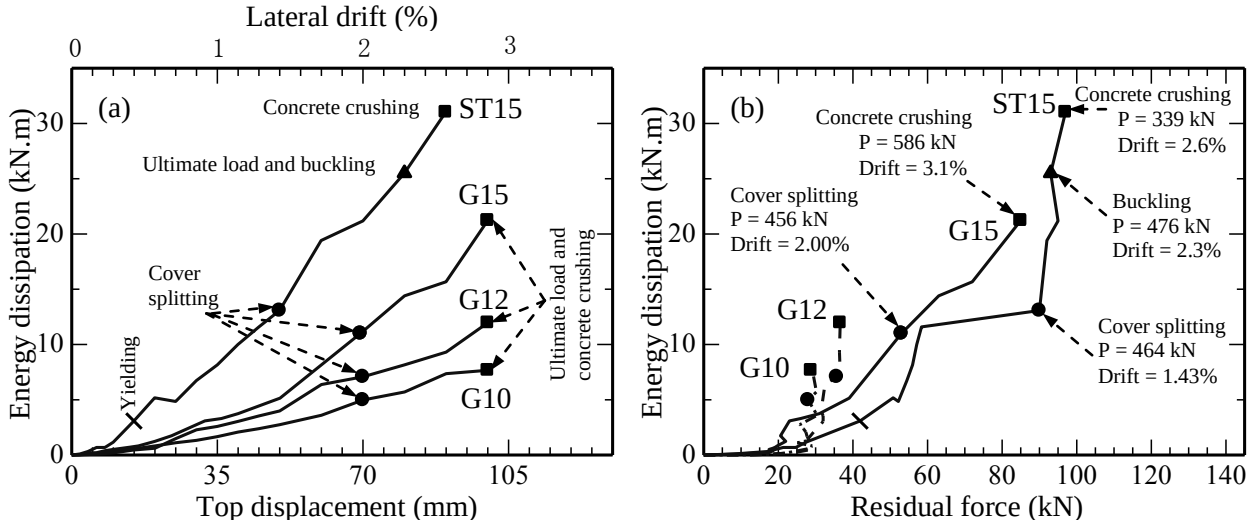

Fig. 3 – Energy Dissipation

In order to compare the effectiveness of the dissipated energy for the different walls, residual force (remaining force at zero displacement) was plotted against the energy dissipated in each cycle (Fig. 3-b). ST15 and G15 had relatively similar dissipated energy until the cover split vertically, at which point, ST15 experienced a sudden increase in residual force (from 58 to 90 kN), leading to the increase in calculated dissipated energy. The increase in G15's residual force, however, was almost linear. Such behavior was expected due to the elastic behavior of the FRP bars. Smaller residual force due to higher aspect ratio is clearly noted by comparing G12 and G10 to G15. Nevertheless, it is important to mention that the minimal residual force (or displacement) is due to the capability of self-centering behavior of GFRP-reinforced walls.

The values mentioned reveal a reasonable energy-dissipation capacity for GFRP-reinforced walls. While the steel-reinforced wall was expected to have higher dissipated energy than the GFRP-reinforced walls, due to the large amount of inelastic deformations as the GFRP reinforcement remained elastic until failure, the GFRP-reinforced shear wall exhibited reasonable energy dissipation.

3. Drift Capacity of GFRP-Reinforced Shear Walls

Completing the design steps requires that the value of force modification factor (R) be assessed. Moreover, quantifying the force modification factor for the tested GFRP-reinforced walls requires that the envelope curve of the load–displacement response of the tested walls be idealized to a bilinear relationship. Although seismic-force modification factors are intended for building systems, the hypothesis herein is based on the response of individual GFRP-reinforced shear walls representing overall building response. This hypothesis was proved to be relevant in past research (Ghorbani-Renani et al. 2009, Shedid et al. 2011). Therefore, the response of individual walls can, to a great extent, represent the response of a building in which the effect of slab coupling between the walls is neglected. Accordingly,

idealizing the actual nonlinear load–displacement response of the tested GFRP-reinforced shear walls is discussed in the following section.

3.1. Idealized Load–Displacement Response

The idealized load–displacement response was obtained based on the envelope curve of the hysteretic load–displacement response. To generate the bilinear idealization of the test results, the transition from elastic to inelastic deformation should be identified. For steel-reinforced shear walls, the elastic region ends at the yield-deformation point (Δ_y), and the inelastic region ends at the maximum deformation point (Δ_u). For GFRP-reinforced shear walls, the elastic region ends at the start of concrete inelasticity (Δ_e), i.e., concrete deterioration at the compressed end of the wall, and the inelastic region ends at the maximum deformation point (Δ_u). The major difference between steel- and GFRP-reinforced shear walls is the absence of yielding phenomenon in GFRP bars. For this reason, the transition point between the elastic and inelastic regions in GFRP-reinforced shear walls is defined herein as the virtual yield deformation point (Δ_e), corresponding to the point at which concrete at the wall ends starts to deteriorate under compressive stresses. Accordingly, producing the bilinear idealized curve meant that two deformation points had to be well defined for each wall specimen: Δ_y or Δ_e and Δ_u. Based on the reviews of existing idealization methods for shear walls as well as data-interpretation procedures for nonlinear testing (Park 1989), the authors decided to incorporate the equivalent energy elastic-plastic (EEEP) bilinear idealization method (Fig. 4). This approach was selected because it has been commonly applied to many types of shear walls (concrete and steel systems, timber, log, sheet-steel sheathing, and masonry shear walls), including those with load–displacement responses similar to GFRP-reinforced shear walls (Branston et al. 2005, Rogers et al. 2011, Shedid et al. 2009, Kessler 2010). The definitions of inelastic displacement (Δ_e) and displacement at ultimate load (Δ_u) were modified for the GFRP-reinforced shear walls, as discussed below.

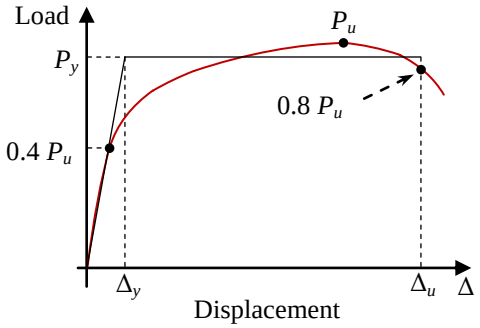

Fig. 4 – Method to Estimate Idealized Load–Displacement Curves

In a practical definition based on an experimental standpoint, a shear wall starts experiencing inelastic deformation when it loses its self-centering behavior (cracks no longer close and realign during unloading) and when the wall becomes permanently deformed. The steel-reinforced shear wall (ST15) lost its self-centering behavior after the yielding of the first longitudinal bar in the boundary at Δ_y = 15 mm. This contrasts with the GFRP-reinforced shear walls, for which Δ_e ranged between 40 and 50 mm at concrete compressive strains ranging between 0.003 and 0.0035. At that point, permanent deformations were initiated and self-centering behavior was completely lost at almost Δ_e = 70 mm, which was associated with the vertical splitting of the concrete cover.

The ultimate displacement (Δ_u) of steel-reinforced shear walls is generally defined as a 20% loss of ultimate lateral strength (NBCC 2010). On the other hand, the actual ultimate displacement in the ends of GFRP-reinforced shear walls occurs at the ultimate lateral strength at which the transverse reinforcement ruptures and longitudinal reinforcement fractures under compression ($\Delta_{capacity}$). In this study, however, the maximum allowable displacement corresponding to an earthquake (Δ_u) for the GFRP-reinforced shear walls was defined to be less than the actual ultimate displacement capacity ($\Delta_{capacity}$) to maintain a conservative value and to avoid collapse. This maximum allowable limit of Δ_u was equal to a value of 87.5 mm, corresponding to 2.5% drift, which is the maximum allowed drift under seismic loads according to ASCE7 (2010), UBC (1988), and NBCC (2010). Confinement details should be considered in the

design procedure based on the concrete compressive strain attained at the suggested value of Δ_u (2.5% drift). Based on the determination of Δ_y, Δ_e, and Δ_u from the experimental results in this study, the idealized load–displacement curves were obtained considering a well-defined initial stiffness, maximum allowable displacement, and equivalent-energy approach. The initial stiffness was taken equal to the secant stiffness at the first major crack, which corresponded approximately to 40% of the ultimate load for the steel- and GFRP-reinforced walls (Figs. 5-a, b, c, and d). The idealized load–displacement curves were obtained using the equivalent-energy approach. The equivalent-energy approach balances areas between the actual results and bilinear idealization.

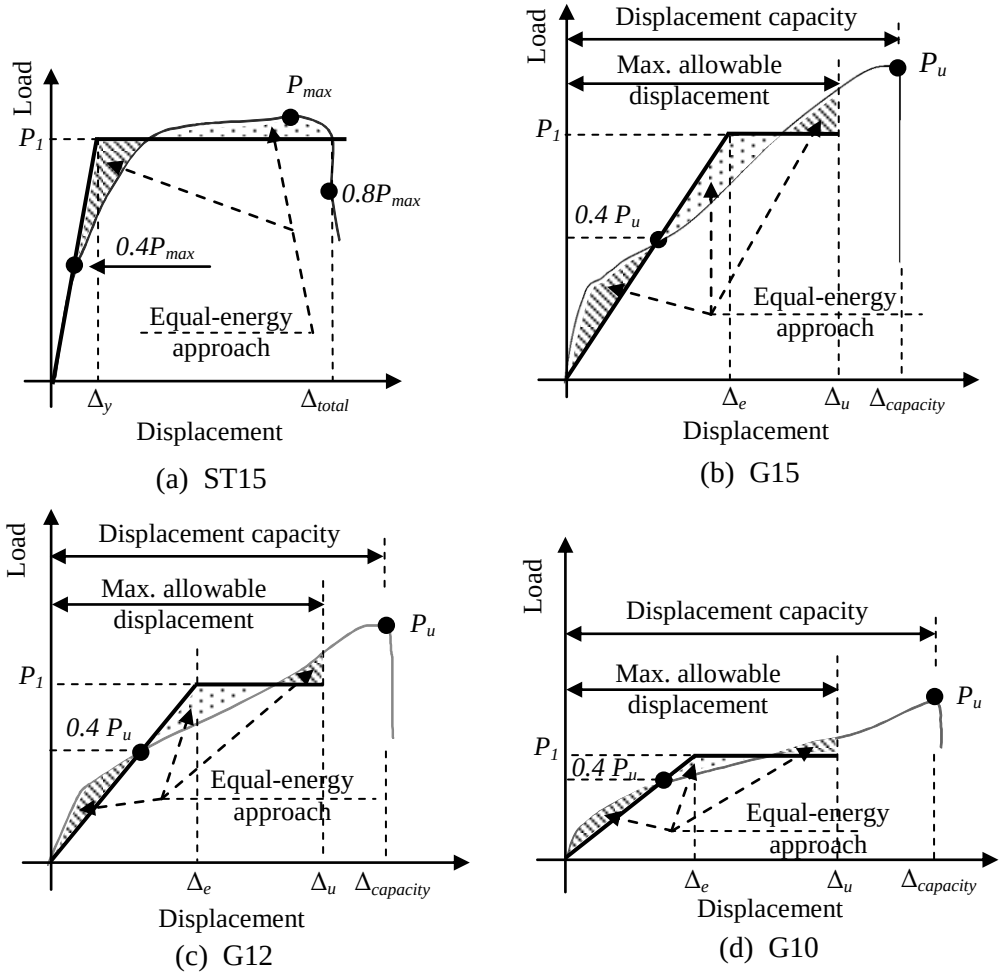

Fig. 5 – Idealized load–displacement curves for tested wall specimens

As shown in Fig. 5, the idealized load–displacement curves consist of two portions: the elastic limit, corresponding to Δ_y for ST15 and Δ_e for GFRP-reinforced shear walls, and the inelastic deformation part up to Δ_u. The elastic limit corresponds to the yielding point in ST15, which was determined to be Δ_y = 14.69 mm from the idealized curve and Δ_y = 15 mm based on the experimental results. The idealized curve well predicted the yield displacement (Δ_y) for ST15. For the GFRP-reinforced shear walls, the elastic displacements (Δ_e) corresponding to the virtual yield point were 53.6, 45.1, and 41.5 mm from the idealized curves of G15, G12, and G10, respectively. Similar values (virtual yield points) ranging between 40 and 50 mm were obtained from the experimental envelope curves of the GFRP-reinforced shear walls at concrete compressive strains ranging between 0.003 and 0.0035. The aforementioned comparison of the displacement at the end of the elastic stage (Δ_y and Δ_e for steel- and GFRP-reinforced shear walls, respectively) to the experimental results and the values obtained based on the idealized curve implies that the method used to generate the idealized curve was precise. Accordingly, the generated idealized curve is considered to be adequate to obtain the force modification factor (*R*) for GFRP-reinforced shear walls.

3.2. Force Modification Factor (*R*)

The design lateral load is lower than the equivalent lateral force, representing elastic response by a force modification factor (*R*). NBCC (2010) views it as a ductility- and overstrength-related force modification factor (R_d and R_o). In CSA S806 (2012), considering the lack of research on the hysteretic behavior of FRP-reinforced members, the design lateral load is determined based on R_d and R_o being equal to unity.

The experimental results of our study showed that the GFRP-reinforced shear walls were able to dissipate energy (Fig. 3). This behavior is a step toward more research on studying the behavior of FRP-reinforced members in resisting seismic loads. Accordingly, there is a need to assess the values of force modification factors (R_d and R_o), since setting them to unity is very conservative. Inelastic time–history analysis indicates that the structure behavior depends on the structure natural period. It was observed that structures with natural periods greater than the maximum elastic spectral response evidenced a maximum displacement similar to those obtained from an elastic system with equal initial stiffness (Paulay and Priestley 1995). This observation is referred to as the "equal-displacement principle" and is used in steel-reinforced concrete structures. For shorter-period structures, it was found that ductility can be reasonably estimated by equating the energy dissipated by the system (i.e. area under the idealized load–displacement curve) to the energy dissipated by an elastic structure with the same initial stiffness. This approach is referred to as the "equal-energy principle" (Paulay and Priestley 1995). The equal-energy principle was applied in this study to the GFRP-reinforced shear walls, where it was found to be more conservative.

3.2.1. Ductility-Related Force Modification Factor (R_d)

The idealized load–displacement curves for the tested walls (Fig. 5) were used to obtain the ductility-related force modification factor (R_d). In the current design codes, the elastic stage up to Δ_e represents the designed capacity (strength capacity) equal to or exceeding the required factored code-specified seismic forces (P_1), which is the maximum load of the idealized load–displacement curve, as shown in Fig. 5. P_2 is the design seismic force due to an earthquake of the intensity specified for the given seismic map area but corresponds to a fully elastic structural response. P_2 was obtained using the "equal-displacement principle" for the steel-reinforced shear wall, as illustrated in Fig. 6-a, and based on the "equal-energy principle" for the GFRP-reinforced shear walls (Figs. 6-b, c, and d). R_d was calculated as P_2 / P_1. As shown in Table 1, R_d for the GFRP-reinforced shear walls ranged from 1.5 to 1.8 and increased with aspect ratio, while it was equal to 6 for the steel-reinforced shear wall. According to the NBCC (2010), in the case of steel-reinforced seismic-resistant systems, R_d ranges from 5.0 for very ductile systems to 1.5 for systems that are not detailed for ductility (brittle systems). The NBCC (2010) recommended R_d values support the estimated values for the tested steel-reinforced shear wall in this study and support recommending that R_d for GFRP-reinforced shear walls be 1.5.

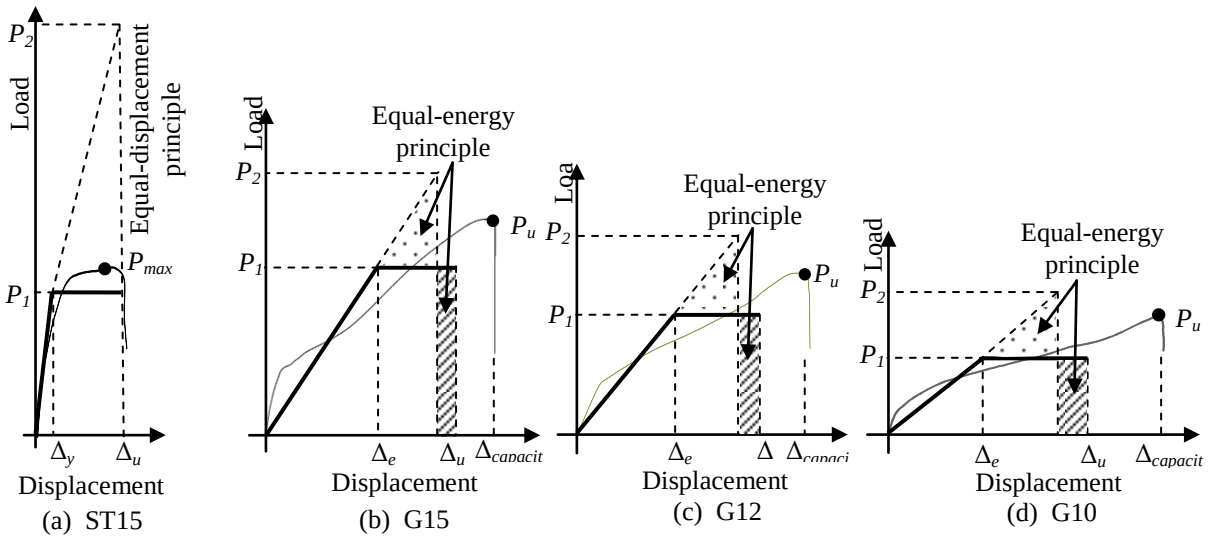

Fig. 6 – Calculation of the ductility-related response modification factor (R_d)

Table 1 – Derivation of force modification factors from experimental results.

Wall	P_u (kN)	Δ^* (mm)	P_1 (kN)	Δ_u (mm)	P_2 (kN)	R_d (P_2/P_1)	R_φ	R_{yield}	R_{sh}	R_o
ST15	476	14.7	439	90	2691	6.13	1.2	1.02	1.25	1.50
G15	586	53.6	462	87.5	695	1.50	1.3	1.03	---	1.37
G12	449	45.1	330		561	1.70				
G10	289	41.5	192		345	1.79				

$*$ Δ_y and Δ_e for steel- and GFRP-reinforced walls, respectively

3.2.2. Ductility-Related Force Modification Factor (R_o)

The NBCC (2010) defines the overstrength-related force modification factor (R_o), for any level of ductility, as the accumulation of probable strength, accounting for all possible factors that contribute to strength based on the dependable portion of the reserve strength, divided by the required seismic design resistance at that level. Mitchell et al. (2003) prescribed the calculation of R_o in the NBCC (2010) as a function of several factors:

$$R_o = R_{size}\ R_\varphi\ R_{yield}\ R_{sh}\ R_{mech} \quad (1)$$

where R_{size} is the rounding of dimension, R_φ is the ratio between nominal and factored material resistances (= $1/\varphi$; φ is the material resistance factor = 0.85 and 0.75 for steel and GFRP bars, respectively), R_{yield} is the ratio of actual yield strength to guaranteed yield strength, R_{sh} is overstrength due to strain hardening, and R_{mech} is the overstrength arising from mobilizing the full capacity of the structure. The value of R_o could be calculated for the GFRP-reinforced shear walls according to the overstrength arising from nominal to factored material resistances (R_φ) and actual to guaranteed specified strengths (R_{yield}; referring to the actual and guaranteed ultimate tensile strengths of GFRP bars). The rest of the factors (R_{size}, R_{sh}, and R_{mech}) were set to unity. Accordingly, the R_o values were 1.5 and 1.37 for the steel- and GFRP-reinforced shear walls, respectively (Table 1).

Generally, based on the aforementioned discussion, GFRP-reinforced shear walls can be considered as limited ductile structures according to CEN (2005) or as shear-wall concrete systems according to the NBCC (2010) with the force modification factors R_d = 1.5 and R_o = 1.35.

4. Conclusion

Based on the experimental program carried out on GFRP-reinforced shear walls compared to a steel-reinforced shear wall, definitions were proposed for elastic and maximum allowable deformations. Idealized curves were obtained and strength reduction factors were assessed. The main findings can be summarized as follows:

1. The GFRP-reinforced shear walls reached similar drift capacities to the steel-reinforced shear wall, with a large elastic portion of deformation followed by a relatively small portion of inelastic deformation.
2. The transition point between the elastic and inelastic regions of the GFRP-reinforced shear walls was defined as the virtual yield deformation point (Δ_e), corresponding to the point at which concrete starts to deteriorate under compressive stresses.
3. The maximum allowable deformation (Δ_u) of the GFRP-reinforced shear walls was estimated as corresponding to 2.5% drift, which is the maximum allowed drift under seismic loads in the NBCC (2010). This conservative value was defined to be always smaller than the actual ultimate displacement capacity ($\Delta_{capacity}$).
4. The force modification factors (R_d and R_o) were suggested to be taken as 1.5 and 1.3, respectively, for the GFRP-reinforced shear walls.

The definitions presented for the virtual yield deformation point (Δ_e) and maximum allowable deformation (Δ_u) and estimation of force modification factors will be used to design GFRP-reinforced shear walls with adequate drift capacity.

5. Acknowledgements

The experimental study was conducted with funding from the Tier-1 Canada Research Chair in Advanced Composite Materials for Civil Structures. The assistance of the technical staff of the new Canadian Foundation for Innovation (CFI) structural lab at the University of Sherbrooke's Department of Civil-Engineering is also acknowledged.

6. References

ACI Committee 318, "*Building Code Requirements for Structural Concrete and Commentary* (ACI 318-08)," ACI, Farmington Hills, MI, 2008, 473 pp.

ACI Committee 440, "*Guide for the Design and Construction of Concrete Reinforced with FRP Bars* (ACI 440.1R-06)," ACI, Farmington Hills, MI, 2006, 44 pp.

ADEBAR, Perry, MUTRIE, James, DEVALL, Ronald, "Ductility of concrete walls: the Canadian seismic design provision 1984 to 2004," *Canadian Journal of Civil Engineering*, Vol. 32, No. 6, 2005, pp. 1124-1137.

ASCE, "Minimum design loads for buildings and other structures," *ASCE 7*, Reston, VA, 2008.

BRANSTON, Aaron, BOUDREAULT, Felix, ROGERS, Colin, "Method for the Design of Light Gauge Steel Frame / Wood Panel Shear Walls," *Advances in Steel Structures*, *Elsevier*, Vol. II, 2005, pp. 1347-1352.

CAN/CSA A23.3-04, "Design of Concrete Structures Standard," *Canadian Standards Association*, Mississauga, Ontario, Canada, 2004, 240 PP.

CAN/CSA S806-12, "Design and construction of building components with fiber-reinforced polymers," *Canadian Standards Association*, Mississauga, Ontario, Canada, 2012, 208 pp.

CARDENAS, Alex, HANSON, John, CORLEY, Gene, HOGNESTAD, Eivind, "Design Provisions for Shear Walls," *ACI Journal*, Vol. 70, No. 3, 1973, pp. 221-230.

DUFFEY, Todd, FARRAR, Charles, GOLDMAN A, "Low-Rise Shear Wall Ultimate Drift Limit," *Earthquake Spectra*, Vol. 10, No. 4, 1994, pp. 655-674.

FINTEL, Mark, "Performance of Buildings with Shear Walls in Earthquakes of the Last Thirty Years," *PCI Journal*, Vol. 40, No. 3, 1995, pp. 62-80.

Uniform building code (UBC),"International conference of building officials," Whittier, California, 1985, 709 pp.

GHORBANI-RENANI, Iman, VELEV, I. N. , TREMBLAY, Robert, PALERMO, Daniel, MASSICOTTE, Bruno, LÉGER, Pierre, "Modeling and Testing Influence of Scaling Effects on Inelastic Response of Shear Walls," *ACI Structural Journal*, Vol. 106, No. 3, 2009, pp. 358-367.

KESSLER, Samantha, "*A Study of the Seismic Response Modification Factor for Log Shear Walls*," M.Sc. Thesis, Kansas State University, 2010, 113 pp.

MITCHELL, Danial, TREMBLAY, Robert, KARACABEYLI, Erol, PAULTRE, Patrick, SAATCIOGLU, Murat, ANDERSON, Donald, "Seismic force modification factors for the proposed 2005 edition of the National Building Code of Canada," *Canadian Journal of Civil Engineering*, Vol. 30, 2003, pp. 308-327.

MOHAMED, Nayera, FARGHALY, Ahmed Sabry, BENMOKRANE, Brahim, NEALE, Kenneth, "Experimental Investigation of Concrete Shear Walls Reinforced with Glass-Fiber-Reinforced Bars under Lateral Cyclic Loading," *ASCE J. Compos. Constr.*, Vol. 18, No. 3, 2014, 04014001.

National Building Code of Canada (NBCC), "Canadian Commission on Building and Fire Codes," *National Research Council of Canada*, 2010, Canada.

PARK, Robert, “Evaluation of Ductility of Structures and Structural Assemblages from Laboratory Testing,” *Bulletin of the New Zealand National Society for Earthquake Engineering*, Vol. 2, No. 3, 1989, pp. 155-166.

PAULAY Thomas. PRIESTLEY M. J. N, “Seismic Design of Reinforced Concrete and Masonry Buildings,” *John Wiley and Sons*, 1995, 735 pp.

ROGERS, Colin, BALH, Nisreen, ONG-TONE, Cheryl, SHAMIM, Iman, DABREO, Jamin, “Development of Seismic Design Provisions for Steel Sheet Sheathed Shear Walls.” *ASCE*, *Proceedings of the Structures Congress,* Las Vegas, Nevada, 2011, pp. 676-687.

SALONIKIOS, Thomas, KAPPOS, Andreas, TEGOS, Ioannis, PENELIS, Georgios, “Cyclic Load Behavior of Low-Slenderness Reinforced Concrete Walls: Failure Modes, Strength and Deformation Analysis, and Design Implications.” *ACI Structural Journal*, Vol. 97, No. 1, 2000, pp. 132-142

SHEDID, Marwan, El-Dakhakhni, Wael, DRYSDALE, Robert, “Behavior of fully grouted reinforced concrete masonry shear walls failing in flexure: Analysis,” *Engineering Structures*, *Elsevier,* Vol. 31, 2009, pp. 2032-2044.

SHEDID, Maewan, EL-DAKHAKHNI, Wael, DRYSDALE, Robert, “Seismic Response Modification Factors for Reinforced Masonry Structural Walls,” *ASCE J. of Performance of Constructed Facilities*, Vol. 25, No. 2, 2011, pp. 74-86.